Available online at www.sciencedirect.com
ScienceDirect
Polymer 48 (2007) 5839–5849
polymer
www.elsevier.com/locate/polymer

Synthesis, characterization, and energy transfer studies of dye-labeled poly(butyl methacrylate) latex particles prepared by miniemulsion polymerization

Ghasem R. Bardajee, Cedric Vancaeyzeele, Jeffrey C. Haley, Alice Y. Li, Mitchell A. Winnik*

Department of Chemistry, University of Toronto, 80 St. George Street, Toronto, Ontario, Canada M5S 3H6

Received 8 June 2007; received in revised form 26 July 2007; accepted 28 July 2007
Available online 3 August 2007

Abstract

Poly(butyl methacrylate) (PBMA) latex particles have been copolymerized with new fluorescent naphthalimide dyes by miniemulsion polymerization. A new pair of naphthalimide dye monomers was synthesized and copolymerized with butyl methacrylate (BMA) via miniemulsion polymerization, producing approximately 80 nm diameter particles with a narrow size distribution. We were able to prepare polymers with molecular weights in excess of 100,000 g/mol. We also prepared 30,000 g/mol polymers using 1-dodecanethiol as a chain transfer agent. GPC and UV characterization suggest that nearly all of the dye monomers were incorporated into the PBMA polymer chains. The polymerized naphthalimide dyes can be used as a donor–acceptor pair for fluorescence resonance energy transfer (FRET) experiments. The analysis of FRET experiments is complicated by the slightly non-exponential decay of the donor naphthalimide dye. We propose a simple method to deal with this non-exponential behavior in the data analysis. Using our approach, we find that the Förster radius (R_o) between the donor and the acceptor dyes incorporated in the PBMA latex is 3.8 nm. This value is similar to the 3.6 nm Förster radius of a comparable model dye pair in ethyl acetate obtained by a different method.

Keywords: Miniemulsion; FRET; Naphthalimide

1. Introduction

In this paper we examine the spectroscopic properties of two new polymerizable dye derivatives that can serve as a donor–acceptor pair for fluorescence resonance energy transfer (FRET) measurements in polymer films. These dyes have maximum wavelength of donor emission and acceptor absorbance to the red of 400 nm, making the FRET experiments much less sensitive to background emission from polymer additives or impurity fluorescence that is often problematic when one uses donor dyes that are excited at 300 nm. We are particularly interested in using these dyes for the study of polymer diffusion in latex films. Thus we describe the incorporation of these dyes into poly(butyl methacrylate) (PBMA) latex particles synthesized by miniemulsion polymerization. In films of this polymer, the fluorescence decay of the donor dye shows a small deviation from an exponential profile. We examine the consequences of this deviation on the analysis of FRET experiments in PBMA films.

Latex dispersions are commonly used in paints and coatings [1]. Elucidating the details of latex film formation remains an important challenge, and will aid the development of new environmentally friendly coatings. The current view is that the conversion of a latex dispersion into a mechanically coherent coating can be broken down into three steps. In the first step, the dispersion dries, bringing the latex particles into contact. In the second step, the particles deform, filling space by forming polyhedral cells. In the third step, polymer segments diffuse across the cell–cell interface, forming entanglements that build up adhesion strength between cells. This

* Corresponding author. Tel.: +1 416 978 6495; fax: +1 416 978 0541.
E-mail address: mwinnik@chem.utoronto.ca (M.A. Winnik).

0032-3861/$ - see front matter © 2007 Elsevier Ltd. All rights reserved.
doi:10.1016/j.polymer.2007.07.065

third step is crucial for the formation of a strong coating. Our group has a long-standing interest in using FRET experiments to study the diffusion of polymer segments across these cell–cell interfaces [2].

In a typical energy transfer experiment on latex film formation, we prepare latex particles with donor and acceptor dyes incorporated covalently along the polymer backbone. Our general strategy is to use a dye that is polymerizable and to copolymerize small amounts of this dye monomer in the latex. In most of our experiments, phenanthrene (Phe) was used as the donor dye and anthracene (An) was used as the acceptor dye [3]. For experiments on poly(vinyl acetate) (PVAc) latex particles, we employed 4-(*N*,*N*-dimethylamino)benzophenone (NBen) as the acceptor dye, since anthracene derivatives strongly inhibit VAc polymerization. One of the fortunate side effects of this change in acceptor dye was that the characteristic distance for energy transfer (Förster radius, R_o) is larger for the Phe–NBen pair ($R_o = 2.5$ nm) than that for the Phe–An pair ($R_o = 2.2$ nm). This apparently small increase in Förster radius allows us to use far less acceptor dye monomer in experiments (0.3 mol% NBen, compared with 1.0 mol% An) [4–11]. Reducing the overall amount of dye in the system minimizes the potential risk of changing latex properties with the dye.

As mentioned in the opening paragraph, sometimes energy transfer experiments on latex polymer films can be affected by background emission from additives or impurities in the polymer. This emission is especially problematic for excitation at short wavelengths (for example, at 300 nm). New donor–acceptor dye pairs that operate at longer wavelengths are one way to work around these problems. A survey of the literature suggested that 1,8-naphthalimide derivatives might serve our purposes. 1,8-Naphthalimide derivatives are a well known class of compounds that have a wide range of applications for synthetic polymers and textile materials, in fluorescent solar energy collectors, as liquid–crystal additives, as electro-optically sensitive materials, in laser technology and as fluorescent markers in medicine and biology [12]. These dyes are relatively easy to synthesize, and the synthesis can be adapted to create polymerizable dyes. Certain 1,8-naphthalimide derivatives have emission and absorption spectra that indicate that they might be useful as donor–acceptor pairs. Our goal is to chemically incorporate these dyes covalently along the polymer backbone.

Miniemulsion polymerization [13,14] is a convenient way to incorporate dyes of poor water solubility into polymer nanoparticles. Miniemulsions are relatively stable submicron (50–500 nm) dispersions of oil in water prepared by homogenizing a system containing oil, water, surfactant, and a costabilizer. The costabilizer is a species with very low water solubility, such as hexadecane, cetyl alcohol or lauryl methacrylate. It acts as an osmotic stabilizer against Ostwald ripening [15–17]. The monomer droplets of nanometer dimensions are created by subjecting the reaction mixture to strong shearing forces. The surfactant provides protection for the droplets against coalescence. Antonietti and Landfester [14], as well as Schork et al. [18], have published recent reviews on miniemulsion polymerization. One of the main advantages of miniemulsion polymerization over traditional emulsion polymerization is that problems associated with transport through the aqueous phase of reactants with limited water solubility are eliminated. In a miniemulsion polymerization, under ideal circumstances, the monomer droplets are small, homogeneous in size and kinetically stable over the reaction time. As they are polymerized, they conserve their identity and yield latex particles. Landfester et al. [19] have shown by a combination of conductivity, surface tension and small angle neutron scattering (SANS) experiments that a one-to-one copy from monomer droplets to polymer particles can be achieved. Under these conditions, each droplet corresponds to a nanoreactor undergoing bulk polymerization [20]. This concept has been widely used to prepare polymer particles containing different kinds of hydrophobic species, such as dyes [11,21].

Here we describe a new pair of polymerizable donor and acceptor co-monomers (**4a** and **4b**) based on the 1,8-naphthalimide nucleus for energy transfer experiments in PBMA latex films. Both the donor (D) and the acceptor (A) labeled latex particles were prepared by miniemulsion polymerization. The donor- and acceptor-labeled latex samples were prepared in the presence of 1 wt% of the desired dye and the molecular weights of the polymers were controlled using a chain transfer agent in the polymerization process. The incorporation and amount of dye in the polymer chains were confirmed by GPC traces and UV measurements in latex samples. We carried out energy transfer experiments to measure the Förster radius for the donor–acceptor pair in PBMA films. These experiments demonstrate that this dye pair will be useful for energy transfer studies of latex film formation.

The remainder of this paper consists of three sections. First, we present the experimental details of the dye monomer synthesis, miniemulsion polymerization, characterization, and fluorescence experiments. Next, we present the results of our FRET experiments, followed by a brief summary.

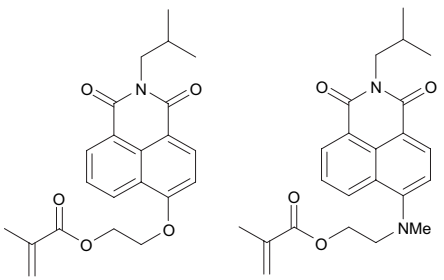

4a **4b**

2. Experimental

2.1. Materials

The syntheses of compounds **2**, **3a** and **3b** are reported elsewhere [22]. Details for the synthesis of the methacrylate esters **4a** and **4b** are provided in Supplementary data.

2.2. Latex synthesis

The recipes used to synthesize dye-labeled poly(butyl methacrylate) particles is given in Table 1. Dye monomer (40 mg, 1 wt% monomer) was dissolved in a mixture of butyl methacrylate (BMA, 3.8 g, 26.70 mmol), and lauryl methacrylate (LMA, 0.2 g, 7.85×10^{-4} mol). For two samples, a chain transfer agent (1-dodecanethiol, $C_{12}SH$, 28 mg, 141 mmol, 0.5 mol% based on total monomers) was used to control the molecular weight of the polymer. These samples are referred to as "low-M samples" whereas the chain transfer agent-free samples are referred to as "high-M samples". As soon as the dye was dissolved, this homogeneous phase was mixed with the aqueous phase composed of deionized water (16 g), sodium dodecyl sulfate (SDS, 0.16 g, 0.55 mmol) and sodium bicarbonate ($NaHCO_3$, 0.08 g, 0.95 mmol). The mixture was emulsified under magnetic stirring for 15 min and then the miniemulsion was prepared by ultrasonication with a Branson Digital sonifier model 450 at 60% amplitude for 4 min (1 s pulse on, 2 s pulse off). During this step the mixture was cooled with ice. Then, the miniemulsion was transferred to a three neck-flask reactor equipped with a condenser and mechanical stirring. The reaction mixture was heated to 80 °C, degassed by purging with N_2 and initiated by the addition of potassium persulfate (KPS) (40 mg, 1.48×10^{-4} mol) in water (2 mL). The reaction mixture was heated with stirring for 9 h at 80 °C and then allowed to cool to room temperature. The particles obtained were coagulum free. We denote all latexes by their nominal number average molecular weight (in kg/mol, gel permeation chromatography (GPC), polystyrene standards) followed by a superscript indicating what dyes have been used to label the particle (e.g. PBMA-450^{A} has $M_n = 450{,}000$ g/mol and is acceptor-labeled).

2.3. Instrumentation

Molecular weights and molecular weight distributions (PDI, polydispersity index) were measured by gel permeation chromatography (GPC) at 22 °C using polystyrene as molar mass standards. These experiments were performed with a Viscotec VE 2001 solvent/sample module, Styragel columns HR-1 and HR-5E, a Waters 480 tunable UV–vis absorbance detector ($\lambda_{ex} = 370$ nm for donor-labeled and $\lambda_{ex} = 410$ nm for acceptor-labeled), and a Waters R410 differential refractometer detector. Reagent grade THF was used as the eluent at a rate of 0.6 mL/min. Particle diameter and size distributions (PSD) were measured with a BI90 particle sizer (Brookhaven Instruments Corporation) at a fixed scattering angle of 90°. Differential scanning calorimetric (DSC) experiments were carried out with a Universal V2.6D TA Instruments under N_2 at a scanning rate of 10 °C/min. The sample was cooled to −50 °C and then heated to 150 °C. Afterwards, the sample was cooled down again to −50 °C for a second run over this range of temperature. The glass transition temperatures (T_g) were registered during this last run. Optical absorption spectra were collected at room temperature on a Perkin–Elmer Lambda 25 spectrometer using 1.00-cm quartz cuvettes. Fluorescence spectra were measured with an SPEX Fluorolog-3 spectrofluorometer (Jobin Yvon/SPEX, Edison, New Jersey). Scanning electron microscopic (SEM) images were obtained with a Hitachi HD2000 scanning transmission electron microscope equipped with a cold stage (at −100 °C) operated in the SEM mode. To prepare each sample, a small drop of the diluted latex (1 wt%) was placed onto a carbon-coated copper TEM grid (200 mesh, purchased from SPI supplies). Each sample was dried in air.

The extinction coefficients (at λ_{max}) are $1.21 \times 10^4\ M^{-1}\ cm^{-1}$ (at 365 nm) for the donor monomer dye **4a** and $1.09 \times 10^4\ M^{-1}\ cm^{-1}$ (at 410 nm) for the acceptor monomer dye **4b**.

2.4. Determination of the dye content of the latex polymer

In order to determine the dye content of the labeled PBMA particles, UV measurements were performed on different purified polymer samples. An aliquot (2 mL) of the as-prepared latex was precipitated by the addition of methanol (2 mL). The polymer was recovered by filtration. It was then dissolved in a minimum of CH_2Cl_2 (2 mL) and precipitated in an excess of methanol (200 mL) to remove any free dye. The precipitates were filtered and completely dried in a vacuum oven for 15 h at room temperature. The GPC results showed that there is no free dye in the dried purified polymer samples. UV

Table 1
Recipe for the synthesis of dye-labeled poly(butyl methacrylate) latex by miniemulsion polymerization at 80 °C[a]

Ingredients (g)	High-M samples				Low-M samples		
	Unlabeled	Acceptor dye	Donor dye	Donor/acceptor (1/0.25) dye	Unlabeled	Acceptor dye	Donor dye
H_2O	16	16	16	16	16	16	16
$NaHCO_3$	0.08	0.08	0.08	0.08	0.08	0.08	0.08
SDS	0.16	0.16	0.16	0.16	0.16	0.16	0.16
BMA	3.8	3.8	3.8	3.8	3.8	3.8	3.8
LMA	0.2	0.2	0.2	0.2	0.2	0.2	0.2
$C_{12}SH$	–	–	–	–	0.028	0.028	0.028
Acceptor dye	–	0.040[b]	–	0.02	–	0.040[b]	–
Donor dye	–	–	0.040[b]	0.008	–	–	0.040[b]

[a] The amounts are listed in grams.
[b] 1 wt% based on total monomer.

measurements were then run on measured amounts of dried samples of the purified polymer dissolved in CH_2Cl_2. In a typical procedure, purified PBMA-31^D (low-M) sample (4.639 mg) was dissolved in dichloromethane (3 mL by weight) and the UV spectra were measured. (To make sure that the entire sample was dissolved in dichloromethane, the solution was gently agitated for 1 h.) Using the extinction coefficient of the dye monomer in dichloromethane and the polymer absorbance (0.47 at λ_{ex}), we calculated the amount of dye incorporation into the polymer chains during miniemulsion polymerization.

2.5. Determination of the Förster radius by the spectral overlap method

We used compound **3a** as a model donor and compound **3b** as a model acceptor to determine R_o for the donor–acceptor pair in a solution of ethyl acetate. R_o can be determined from measurable parameters via the relation [23]

$$R_o^6 = \frac{9000(\ln 10)\kappa^2 \Phi_f}{128\pi^5 N_{av} n^4} \int_0^\infty f_D(\lambda)\varepsilon(\lambda)\lambda^4 \, d\lambda \quad (1)$$

where κ^2 is the transition dipole moment orientation factor (2/3 in solution), Φ_f is the fluorescence quantum yield of the donor, N_{av} is Avogadro's number, n is the index of refraction of the solvent (1.37 for ethyl acetate), $f_D(\lambda)$ is the normalized fluorescence spectrum of the donor, and $\varepsilon(\lambda)$ is the extinction coefficient spectrum of the acceptor. In order to determine R_o, we measured Φ_f, $f_D(\lambda)$, and $\varepsilon(\lambda)$.

The quantum yield of compound **3a** in ethyl acetate was measured relative to an aqueous solution of quinine bisulfate in 1.0 N H_2SO_4 (reference sample quantum yield 0.55). Corrected fluorescence spectra of **3a** and the reference solution were taken at known concentrations, and the integrated area under each spectrum was determined. The quantum yield of compound **3a** was determined by the equation

$$\Phi_f = \frac{(1 - 10^{-A_s})F_x n_x^2}{(1 - 10^{-A_x})F_s n_s^2} \Phi_s \quad (2)$$

where A_s is the absorbance of the quinine bisulfate reference solution at the excitation wavelength, A_x is the absorbance of the compound **3a** solution at the same excitation wavelength, F_x and F_s are the integrated areas under the compound **3a** solution and the reference solution, n_x is the index of refraction of ethyl acetate, n_s is the index of refraction of 1.0 N H_2SO_4 (1.34), and Φ_s is the quantum yield of the reference sample. Using Eq. (2), we calculate a quantum yield of 0.78 for **3a** in ethyl acetate.

Absorbance spectroscopy was used to generate the extinction coefficient spectrum of the acceptor dye **3b** in ethyl acetate. The extinction coefficient of compound **3b** is 1.1×10^4 M^{-1} cm^{-1} at the maximum wavelength (407 nm). The overlap integral in Eq. (1) was determined numerically by a standard quadrature approach. Using Eq. (1), we find that $R_o = 3.6$ nm for the model compounds in ethyl acetate.

2.6. Fluorescence decay measurements

All fluorescence decay measurements were carried out on solvent-cast films using a nanosecond time-correlated single photon counting system with a 370 nm NanoLED from IBH as the excitation source. Film samples on small quartz plates were placed in a quartz tube for the measurement. The instrumental response function was obtained using a silica (Ludox™) scattering solution. The donor dye was excited at 370 nm. Its intensity decay was monitored at 405 nm, a wavelength where there is almost no detectable fluorescence from the acceptor. We set the resolution of the instrument's multichannel analyzer at 0.1135 ns per channel; this is well matched for the roughly 5 ns lifetime of the donor dye.

To prepare solvent-cast polymer film samples, the dried sample components were co-dissolved in methylene chloride. Films were cast from these solutions on glass microscope slides. The films were initially air dried for 24 h, followed by drying under vacuum for 15 h. We prepared a number of different samples; the details of sample composition are described in Section 3.

2.7. Data analysis

The fluorescence decays were fitted to several different functions. The donor decay by itself showed small but consistent deviations from an exponential profile. Thus we resorted to fit the donor decay using a stretched exponential function

$$I(t) = A \exp\left[-\left(\frac{t}{\tau}\right)^\beta \right] \quad (3)$$

where A, τ, and β are fitting parameters. The mean relaxation time of a stretched exponential function is calculated with the relation [24]

$$\langle \tau \rangle = \frac{\tau}{\beta} \Gamma\left(\frac{1}{\beta}\right) \quad (4)$$

where $\Gamma(x)$ is the gamma function. In order to fit data from energy transfer experiments, we used a modified Förster equation

$$I(t) = A \exp\left[-\left(\frac{t}{\tau}\right)^\beta - P\sqrt{\frac{t}{\langle \tau \rangle}} \right] \quad (5)$$

where P is a fitting parameter. In fits of Eq. (5), τ and β are fixed at values extracted from the donor-only decay. We assume, as a working hypothesis, that P is related to the acceptor concentration, C_A, and the Förster radius, R_o, by the relation

$$P = \frac{4}{3}\pi^{1.5} R_o^3 C_A \left(\frac{3\kappa^2}{2}\right)^{0.5} \quad (6)$$

where κ is the orientation parameter, fixed such that $\kappa^2 = 0.476$. This expression is rigorously true for a random

distribution of immobile donor and acceptor groups if the decay of donor is strictly exponential.

For each fit, Eq. (3) or (5) was convoluted with the instrumental response function using a quadrature routine. This convoluted decay was fit to the experimental data using the Levenberg–Marquardt algorithm. All of the reported fits were judged to be good, based on the randomness of weighted residual plots and χ^2 values generally less than 1.2.

3. Results and discussion

3.1. Synthesis of dye monomer

The synthesis of donor and acceptor monomer dyes is shown in Scheme 1.

Compound **2** was obtained by the condensation reaction of 4-bromo-1,8-naphthalic anhydride with isobutyl amine in 1,4-dioxane as solvent. In the second step of the synthesis, compound **2** was reacted with an excess amount of a bifunctional nucleophile, either ethylene glycol in the presence of KOH or 2-(methylamino)ethanol in the presence of triethylamine to give compounds **3** [22]. Finally, the desired dye monomers **4a** and **4b** were obtained from the reaction of compounds **3a** and **3b** with methacryloyl chloride.

The normalized UV and fluorescence spectra of the donor and acceptor monomer dyes **4a** and **4b** in dichloromethane are shown in Fig. 1. Due to the charge-transfer nature of the lowest excited state of these dyes, and the stronger electron donating nature of the amine substituent in **4b** relative to the alkoxy substituent in **4a**, there is a red shift in both the UV and the fluorescence spectra of **4b** relative to the corresponding spectra of **4a**.

3.2. Synthesis of dye-labeled poly(butyl methacrylate) latex

A series of latex samples for this study were synthesized by miniemulsion copolymerization of butyl methacrylate and monomer dye. In the experiments reported here, we dissolved

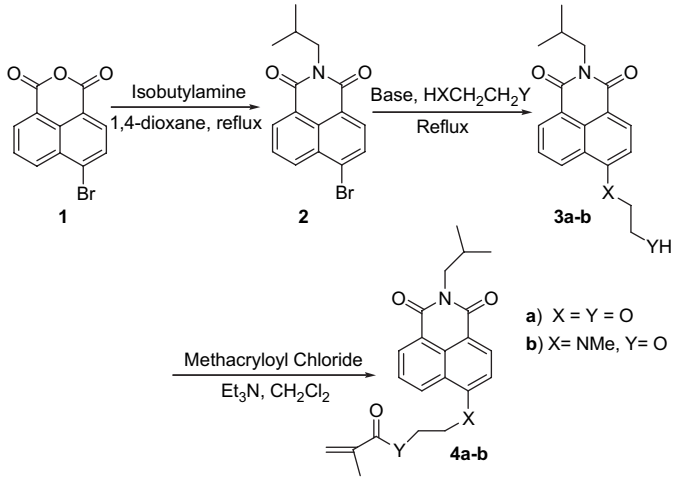

Scheme 1.

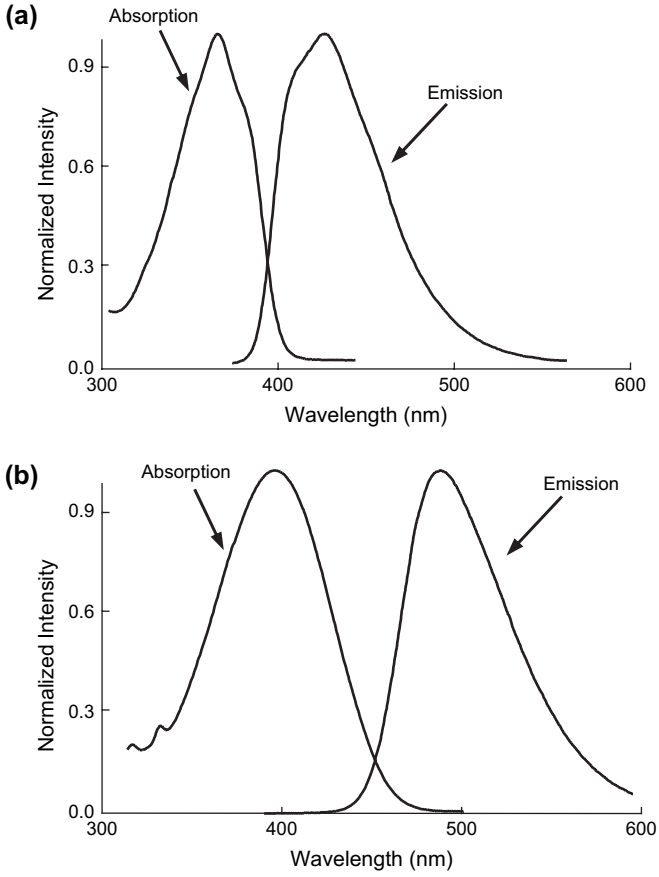

Fig. 1. Normalized absorption and emission spectra of (a) donor monomer **4a** ($\lambda_{ex} = 365$ nm, $\lambda_{em} = 425$ nm) and (b) acceptor monomer **4b** ($\lambda_{ex} = 410$ nm, $\lambda_{em} = 500$ nm) in CH_2Cl_2.

the monomer dye (1 wt% of total monomer) in butyl methacrylate containing 5 wt% (based on total amount of monomer) lauryl methacrylate (LMA) as a polymerizable osmotic costabilizer. After sonication, the monomer droplets were polymerized into PBMA particles using KPS as a water-soluble initiator. The recipes and monomer compositions of all the samples discussed in this paper are reported in Table 1. The characteristics of the particles obtained are summarized in Table 2.

The first three samples, the "high-M samples", were prepared without a chain transfer agent. The particle mean diameters ranged from 65 nm for the donor/acceptor (1/0.25) doubly labeled PBMA latex (PBMA-281DA) to 80 nm for the donor-labeled PBMA latex (PBMA-360^{D}). The particle size distribution for each set of particles was relatively narrow. Molecular weights (M_n) of the polymers and the polydispersity indices were measured by GPC and the values reported are based upon polystyrene standards. For the high-M samples (prepared in the absence of $C_{12}SH$), we found $M_n = 400{,}000$ g/mol (PDI = 2.7) for unlabeled PBMA, $M_n = 450{,}000$ g/mol (PDI = 3.0) for acceptor-labeled PBMA, $M_n = 360{,}000$ g/mol (PDI = 3.0) for the donor-labeled PBMA and $M_n = 281{,}000$ g/mol (PDI = 3.3) for the donor/acceptor (1/0.25) doubly labeled PBMA. The similarity in molecular weights and the PDI values indicates that inclusion of the dyes in the

Table 2
Characteristic of the poly(butyl methacrylate) latex, synthesized by miniemulsion polymerization at 80 °C

Sample	M_n[a] (kg/mol)	PDI[a]	T_g[b] (°C)	d_Z[c] (nm)	PSD[c]
High-M					
Unlabeled (PBMA-400)	400	2.7	–	79	0.04
Acceptor-labeled (PBMA-450^A)	450	3.0	31	78	0.04
Donor-labeled (PBMA-360^D)	360	3.0	32	80	0.02
Donor/acceptor-labeled (1/0.25) (PBMA-280DA)	281	3.3	29	65	0.13
Low-M samples					
Unlabeled (PBMA-30)	30	1.9	–	80	0.03
Acceptor-labeled (PBMA-33^A)	33	2.1	27	78	0.05
Donor-labeled (PBMA-31^D)	31	2.2	26	74	0.05

[a] The number average molecular weight (M_n) and the molecular weight distribution (PDI = M_w/M_n) were measured by GPC (RI detector) using polystyrene as molar mass standards.
[b] Measured by DSC Q100 TA instruments.
[c] The *z*-average particle diameter and the particle size distribution were measured with the BI90 particle sizer.

reaction mixtures have at most a small influence on the free radical polymerization process for the high-M PBMA samples.

The ''low-M samples'' described in Table 2 were synthesized in the presence of C_{12}SH as a chain transfer agent. This chain transfer agent is a good candidate for miniemulsion (or bulk) polymerization with methacrylates, since it has a suitable transfer constant, with C_{tr} equal to 0.678 [25] and fairly low water solubility [26]. The particle diameters were 80 nm, 78 nm and 74 nm for the unlabeled PBMA, the acceptor-labeled (PBMA-33^A) and the donor-labeled (PBMA-31^D) latexes, respectively. The particle size distributions of these samples are narrow (0.05 for the labeled PBMA and 0.03 for the unlabeled PBMA samples). The addition of C_{12}SH leads to lower molecular weight polymers with $M_n = 30{,}000$ g/mol (PDI = 1.9) for the unlabeled PBMA, $M_n = 33{,}000$ g/mol (PDI = 2.1) for the acceptor-labeled PBMA and $M_n = 31{,}000$ g/mol (PDI = 2.2) for the donor-labeled PBMA as reported in Table 2. The molecular weight and the PDI of the labeled low-M PBMA are in the same range as the unlabeled low-M PBMA. Here the dye co-monomers have no detectable influence on the polymerization reaction. As measured by DSC, the glass transition temperatures (T_gs) of the PBMA polymer varied from 26 °C to 32 °C. The two lowest T_g values (27 °C for the acceptor-labeled PBMA and 26 °C for the donor-labeled PBMA) were registered for the low-M polymers synthesized with C_{12}SH.

A few freeze-dried particle samples were also characterized by scanning electron microscopy, with the sample cooled to −100 °C with a cold stage to minimize sample damage during beam exposure. One example (PBMA-360^D) is shown in Fig. S1 in Supplementary data. The sizes seen in the SEM images are consistent with those determined with the BI90 particle sizer.

3.3. Dye distribution and dye content in the latex polymer samples

We used GPC equipped with dual detectors (RI, UV–vis) to test for the presence of the free dye in the latex samples and to examine the uniformity of the dye distribution. In each sample, the signal for the polymer was monitored by the RI trace, and the signal for the dye was monitored by the UV–vis trace at a wavelength corresponding to the maximum absorption of the dyes ($\lambda_{ex} = 370$ nm or 410 nm). The compounds were eluted at volumes consistent with the fact that the UV detector precedes the RI detector. In order to compare the shape of both traces, we shifted the UV trace by a delay volume of 0.25 mL. This delay volume was estimated from the RI and UV traces of a monodisperse polystyrene standard ($M_n = 11{,}600$ g/mol, PDI = 1.03).

Fig. 2 shows the GPC curves of the dye-labeled poly(butyl methacrylate) synthesized by miniemulsion polymerization. In Fig. 2a, we plot the traces of both donor-labeled PBMA latex synthesized with (PBMA-31^D) and without C_{12}SH (PBMA-360^D). Both the UV and the RI GPC traces of the PBMA synthesized in the presence of the chain transfer agent have a maximum at higher elution volume. Thus, the chain transfer agent C_{12}SH effectively lowered the polymer molecular weight. In Fig. 2b, GPC traces of the acceptor-labeled PBMA synthesized with (PBMA-33^A) and without chain transfer agent (PBMA-450^A) are reported. As was the case for the donor-labeled PBMA, both the UV and the RI GPC traces of the acceptor-labeled PBMA synthesized with C_{12}SH (0.5% wt/wt total monomer) have a maximum at higher elution volume, indicating a lower molecular weight.

The miniemulsion polymerization carried out without C_{12}SH generated a high molecular weight polymer ($M_n = 450{,}000$ g/mol and PDI = 3.0) whereas the miniemulsion polymerization carried out with 0.5 wt% C_{12}SH gave a polymer with a lower molecular weight ($M_n = 33{,}000$ g/mol and PDI = 2.1) [27]. The GPC trace of the donor/acceptor doubly labeled PBMA polymer is reported in Fig. 3c. These GPC results confirm that dodecanethiol is a useful chain transfer agent for this miniemulsion polymerization.

For most of the GPC traces of donor-labeled polymer in Fig. 3, there is a small ''bump'' in the UV signal at an elution volume of roughly 22 mL. No corresponding bump in the UV signal for PBMA-450^A or PBMA-33^A is observed (Fig. 3b), although these two samples do exhibit a rise in the RI signal at a similar elution volume (likely due to the elution of injected solvent or another impurity). The bump in the UV signals at 22 mL for donor-labeled polymers most likely represents the signal from unpolymerized dye monomer.

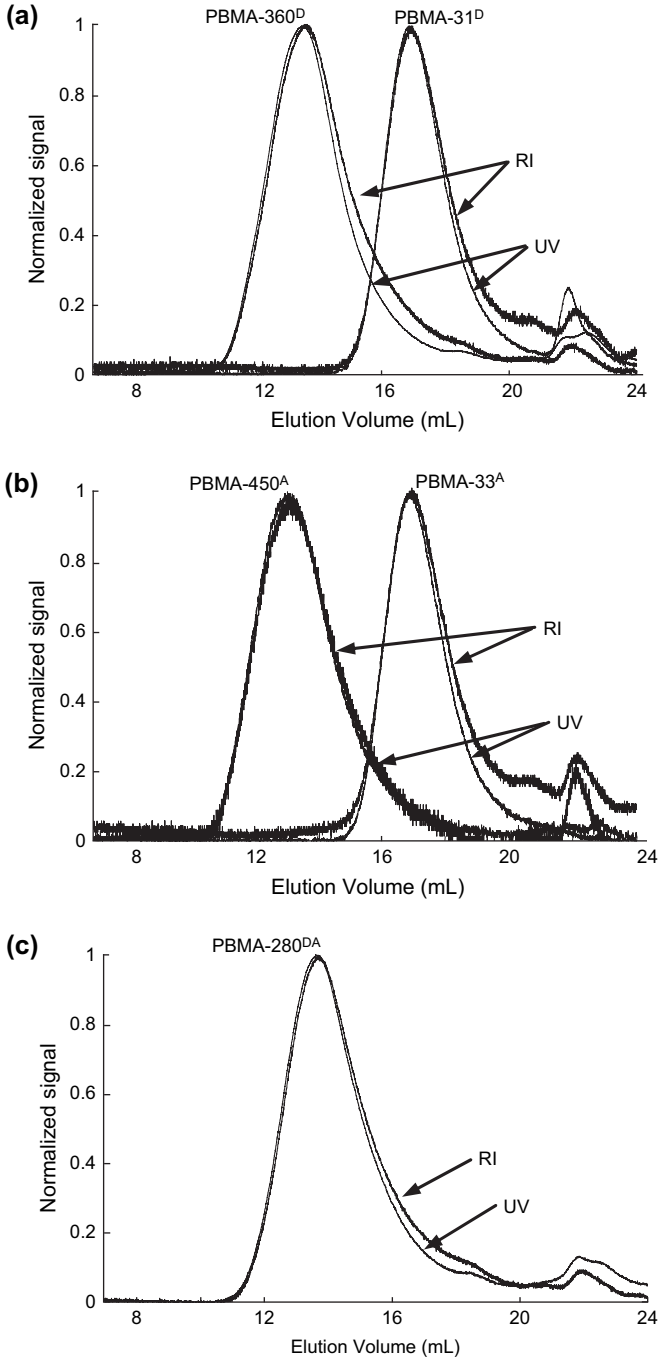

Fig. 2. GPC trace for (a) donor-labeled PBMA latex (with and without chain transfer agent, $C_{12}SH$), (b) acceptor-labeled PBMA latex (with and without $C_{12}SH$), and (c) donor/acceptor (1/0.25) doubly labeled PBMA latex synthesized by miniemulsion polymerization. The UV absorption ($\lambda_{ex} = 370$ nm for the donor or $\lambda_{ex} = 410$ nm for the acceptor) signal and refractive index (RI) signal were normalized and the UV peak was shifted by 0.25 mL to compensate for the fact that the sample passed first through this detector.

Baseline stability issues limit our ability to determine the fraction of free dye in each sample from GPC results alone, but we estimate from the UV traces that only about 5% of the total dye monomer was not covalently attached to the polymer.

We are very much interested in the nature or uniformity of dye distribution in our synthesis: are the dye monomers

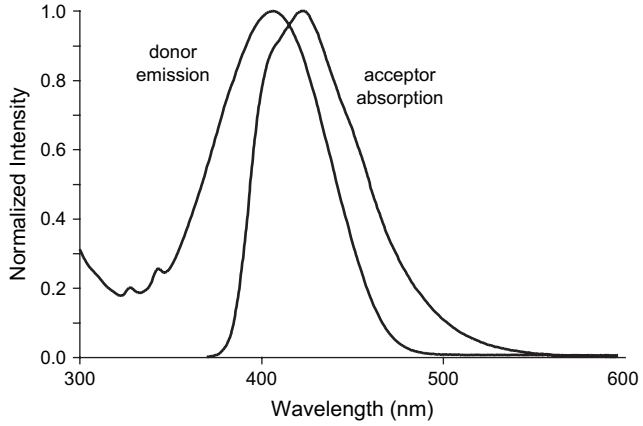

Fig. 3. Normalized emission of donor monomer **4a** (0.44×10^{-7} M) and absorption of acceptor monomer **4b** (10^{-7} M) in CH_2Cl_2.

randomly incorporated along the polymer backbone, or alternatively, do differences in the reactivity of dye monomer and BMA monomer result in a biasing in the labeling process? In Fig. 2a, the RI and UV traces for PBMA-360^D do not overlay perfectly, but instead the RI signal is larger at the high elution volume (low molecular weight) end of the trace. This result suggests that the donor dye is, to a very slight degree, preferentially attached to the higher molecular weight chains in the distribution. We contrast this with the trace for PBMA-450^A (Fig. 2b), where the RI and UV traces overlay perfectly. This supports the tentative hypothesis that acceptor dyes have been randomly incorporated along the PBMA backbone; certainly there is no biasing of the labeling efficiency based on molecular weight. In Fig. 2c, we again see that the UV and RI traces do not overlay at higher elution volumes, indicating that in PBMA-280DA one (or both) of the dyes has been selectively incorporated to higher molecular weight chains (likely the donor dye). Because of difficulties with the RI baseline at high elution volumes, we are unable to make a similar determination for PBMA-31^D or PBMA-33^A.

To determine the dye content of each polymer, we first purified the polymer of any free dye by successive precipitation of the polymer from dichloromethane solution into methanol. Based on the extinction coefficient of the monomer dye, the molar fractions of dye attached to the polymer were calculated (Table 3) from absorption spectra of solutions of the purified polymer.

The mole fraction of dye attached to the PBMA synthesized by miniemulsion polymerization is very similar to the total amount of dye introduced during the polymerization. The efficiency of dye incorporation ranges from 96% for the donor-labeled PBMA without $C_{12}SH$ to 100% for the acceptor-labeled PBMA without $C_{12}SH$. These values are consistent with the qualitative information from GPC traces. The labeling efficiency of the donor-labeled PBMA is not perfect, but more than 96% of the dye is attached to the polymer. Moreover, one has to take into account that low molar mass polymer may have been lost during the polymer purification process, suggesting that the results in Table 3 may slightly underestimate the dye labeling efficiency.

Table 3
Molar fraction of dye attached to the PBMA synthesized by miniemulsion polymerization with (low-M samples) or without (high-M samples) the addition of $C_{12}SH$

Dye-labeled PBMA sample	Dye incorporation[a] (mmol/g of polymer)	Mole fraction of copolymerized dye[a] (%)
PBMA-360^{D}	0.025	96
PBMA-450^{A}	0.025	100
PBMA-280DA	0.013/0.005[b]	97/99[b]
PBMA-31^{D}	0.026	98
PBMA-33^{A}	0.024	97

[a] Determined by UV measurements and based on the total amount of dye introduced during the synthesis.
[b] These numbers refer to donor and acceptor content of polymer chains, respectively, in doubly labeled latex particles.

3.4. Energy transfer experiments in PBMA latex films

The primary goal of these experiments was to determine if the dyes and dye-labeled polymers obtained were suitable for future energy transfer experiments. In Fig. 3 we plot the normalized emission spectrum of the donor monomer **4a** and normalized absorbance spectrum of the acceptor monomer **4b** in CH_2Cl_2. There is considerable overlap between the two spectra suggesting that the dyes should make a suitable donor–acceptor pair for energy transfer experiments. Analysis of the corresponding spectra in ethyl acetate solution by the spectral overlap method led to a value of the characteristic (Förster) energy transfer distance $R_o = 3.6$ nm.

The fluorescence decay of a film of "high-M" donor-labeled PBMA polymer (PBMA-360^{D}) is plotted in Fig. 4a. This decay could not be fitted with a single exponential decay, the best fit gave a $\chi^2 = 2.02$. This fit is also shown in Fig. 4a. The weighted residual plot for the single exponential fit is shown in Fig. 4b.

The decay profile for PBMA-360^{D} gave a much better fit to a stretched exponential function (Eq. (3); $\chi^2 = 1.02$). This fit is shown in Fig. 5a. The resulting fitting parameters were $\tau = 5.3$ ns, $\beta = 0.92$, and $\langle\tau\rangle = 5.5$ ns. The β parameter value indicates a small but detectable deviation from single exponential behavior.

We measured the fluorescence decays of three different donor/acceptor-labeled samples. Fig. 5b presents the fluorescence decay for a film of the high-M doubly labeled (D/A = 1/0.25) PBMA polymer (PBMA-280DA) for which the acceptor concentration is 3.2×10^{-3} nm^{-3} (5.3 mM). For comparison purposes, we have also prepared two blends of polymers separately labeled with donor and acceptor dyes. In order to match the overall concentration of acceptors in the system with the acceptor concentration of the high-M PBMA-280DA, these blends consist of 80 wt% donor-labeled polymer (PBMA-360^{D} or PBMA-31^{D}) and 20 wt% acceptor-labeled PBMA polymer (PBMA-450^{A} or PBMA-33^{A}). Fig. 5c shows the decay for the 80/20 PBMA-31^{D}/PBMA-33^{A} blend and Fig. 5d shows the decay for the 80/20 PBMA-360^{D}/PBMA-450^{A} blend. All three decays were successfully fitted with Eq. (5). We obtained the following P values from the fits: PBMA-280DA, $P = 0.86$ ($\chi^2 = 1.09$); 80/20 PBMA-31^{D}/PBMA-33^{A}, $P = 0.80$ ($\chi^2 = 1.13$); 80/20 PBMA-360^{D}/PBMA-450^{A}, $P = 0.64$ ($\chi^2 = 1.00$). The P values for the low-M blend and the doubly labeled polymer are similar, whereas the P value for the high-M blend is significantly lower. The experimental error in the value of P cannot be more than 10%. To demonstrate this, we refit the 80/20 PBMA-360^{D}/PBMA-450^{A} by forcing $P = 0.58$ and obtained $\chi^2 = 1.25$. Setting $P = 0.69$ for the same sample gives a $\chi^2 = 1.38$. Clearly, χ^2 is a very sensitive function of P. Based on this error analysis, the difference in P between the high-M blend and the low-M blend is significant.

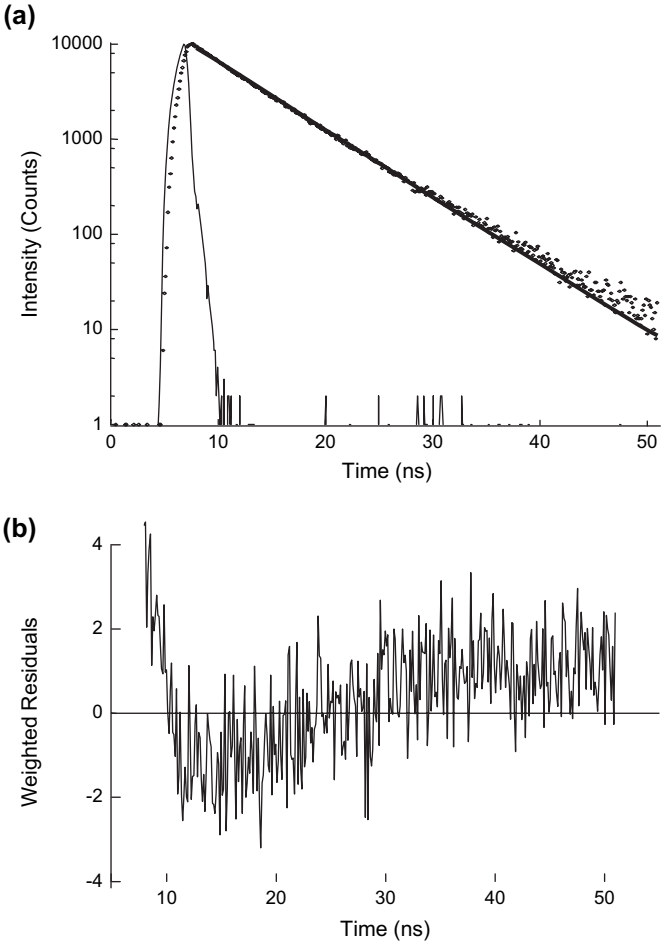

Fig. 4. (a) Fluorescence intensity decay of PBMA-360^{D} fitted to an exponential decay. Plotted are the experimental data (points), the instrumental response function (thin line), and the exponential fit (heavy line). (b) The weighted residual plot for the exponential fit in part (a).

We calculated the energy transfer efficiency (Φ_{ET}) for each of these samples with the relation

$$\Phi_{ET} = 1 - \frac{\int_0^\infty I_{D,A}(t)\mathrm{d}t}{\int_0^\infty I_D(t)\mathrm{d}t} \tag{7}$$

where $I_{D,A}(t)$ and $I_D(t)$ are the fitted intensity decay functions for the donor in the presence and absence of acceptor,

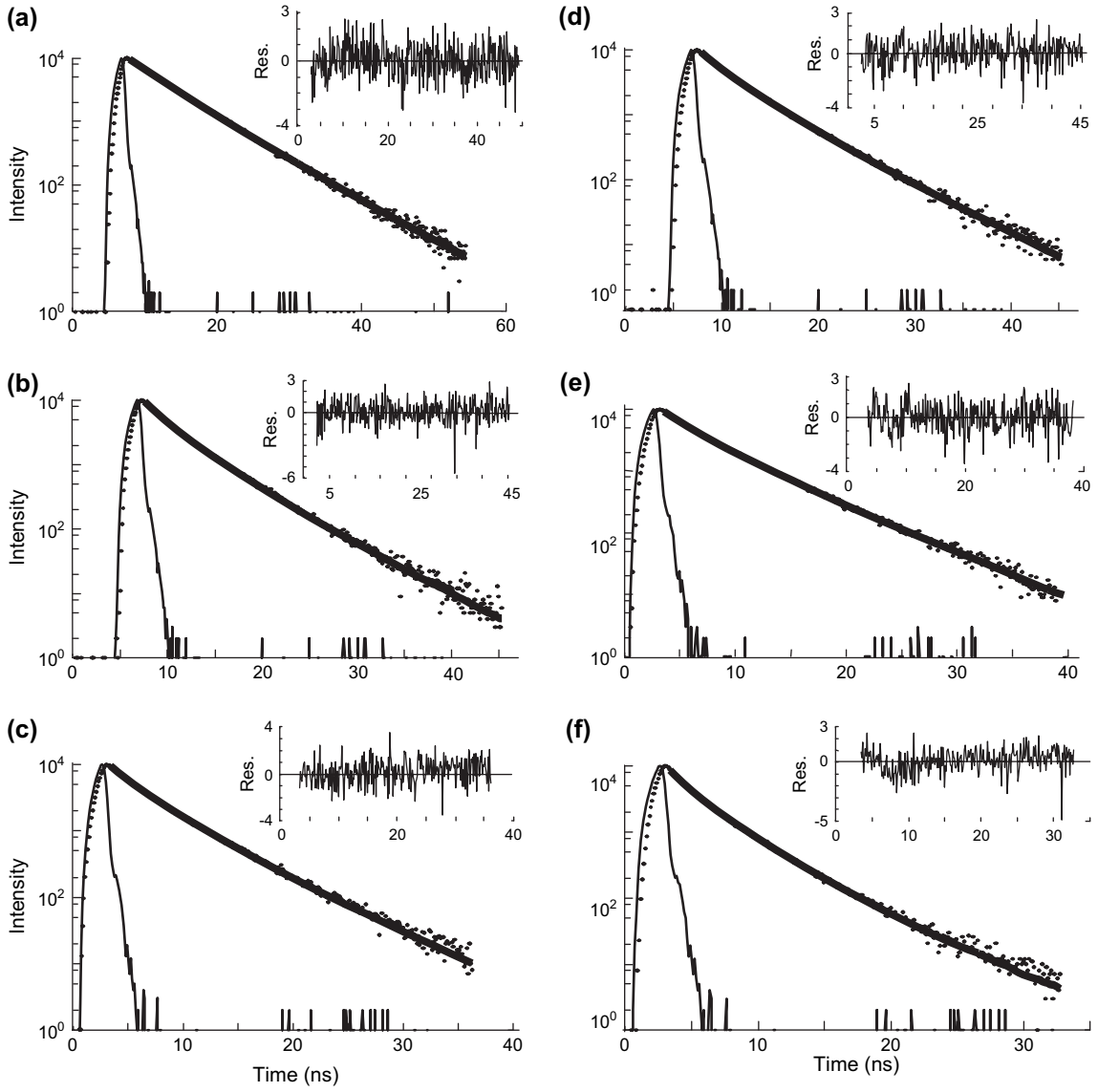

Fig. 5. Selected fluorescence intensity decays and corresponding fits with Eqs (3) and (5). Plotted are the experimental data (points), instrumental response function (thin line), fit (heavy line) and weighted residuals (inset). (a) PBMA-360^{D}, (b) PBMA-280DA, (c) 80% PBMA-31^{D}/20% PBMA-33^{A}, (d) 80% PBMA-360^{D}/20% PBMA-450^{A}, (e) PBMA-360^{D} plus free acceptor dye **4b** $C_A = 1.8 \times 10^{-3}$ dyes nm^{-3} (3.0 mM), and (f) PBMA-360^{D} plus free acceptor dye **4b** $C_A = 4.9 \times 10^{-3}$ nm^{-3} (8.1 mM).

respectively. No simple analytical solution to the integral of Eq. (5) could be found, so the integrals were calculated numerically from the parameters in the fit of Eq. (5). We found that for the doubly labeled polymer $\Phi_{ET} = 0.51$, for the low molecular weight blend $\Phi_{ET} = 0.49$, and for the high molecular weight blend $\Phi_{ET} = 0.42$. The difference between the doubly labeled polymer and the low molecular weight blend is fairly small, whereas Φ_{ET} for the high molecular weight blend is significantly less than what is found with the other two samples. This trend in Φ_{ET} can be rationalized in terms of the "correlation hole effect" [28–30]. The magnitudes of P and Φ_{ET} are very sensitive to the concentration of acceptors within about 5 nm of donor dyes. Polymer chain connectivity effects lead to a local depletion of acceptor-labeled polymer in the immediate vicinity of donor-labeled polymer; this depletion is known as a correlation hole. Both the radius and the depth of this correlation hole increase as polymer molecular weight increases [28]. The correlation hole effect is consistent with the observation that there is less energy transfer in the high-M blend than in the low-M blend.

We also prepared a series of seven samples made up of PBMA-360^{D} and free acceptor monomer **4b**. These samples contained acceptor concentrations ranging from 6.4×10^{-4} nm^{-3} (1.1 mM) to 6.2×10^{-3} nm^{-3} (10.3 mM). The donor decays for these samples were fitted with Eq. (5). Sample fits are shown in Fig. 5e ($C_A = 1.8 \times 10^{-3}$ nm^{-3}) and Fig. 5f ($C_A = 4.9 \times 10^{-3}$ nm^{-3}). The resulting P values are plotted as a function of acceptor concentration in Fig. 6. The fitted P values all fall along a straight line with an intercept at the origin. Using Eq. (6), we obtain $R_o = 3.8$ nm. The fact that the P values

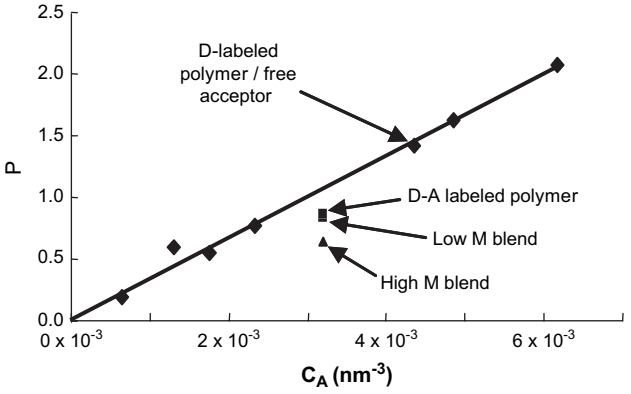

Fig. 6. Plot of P vs. C_A for films containing mixtures of PBMA-360^D and free acceptor monomer **4b**. The line is a fit of these data to Eq. (5). Also shown are P values for films formed from the doubly labeled polymer and for the 80/20 high-M and low-M D- and A-labeled polymer blends.

are a linear function of C_A with a zero intercept helps us to validate our analysis. In effect, using Eq. (5) to fit our data, we have assumed that we can treat the energy transfer process from a donor with a non-exponential decay profile with a single Förster radius; the linear relationship between P and C_A is consistent with this assumption. Further support for our assumption is that the extracted $R_o = 3.8$ nm is very similar to the value of 3.6 nm in ethyl acetate determined using the spectral overlap method (see Section 2).

The P values for the three acceptor-labeled polymer samples are also plotted in Fig. 6. All three data points fall below the line for the free acceptor dye. The correlation hole effect, described above, may account for why the low-M and high-M samples fall below the free dye line in Fig. 6. Free acceptor dye is not expected to be excluded from the donor because the donor is covalently attached to the polymer.

The difference between the doubly labeled polymer and the free acceptor dye system is more surprising. In principle, both systems should be comparable, as both should contain randomly placed donor and acceptor dyes. Based on the single data point of the doubly labeled system, we estimate that $R_o = 3.5$ nm, a value that is considerably less than the 3.8 nm value for the free acceptor system (while this difference may seem small, it is R_o^3 that enters into Eq. (6) relating acceptor concentration to the rate of ET). We can attribute this difference to two possible sources. First, subtle differences in the reactivity of the donor monomer, acceptor monomer, and the BMA monomer might lead to a partial segregation of donor and acceptor labels in the doubly labeled sample. Local segregation of polymerized dye monomer and unlabeled monomer has been reported for miniemulsion polymerization [31], although this system had reactivity ratios between different monomers that were much more poorly matched than what is likely for our methacrylate dye monomers. Some evidence of non-uniform labeling is found in the GPC results for the donor dye, but not for the acceptor dye. A second possibility is that the acceptor absorbance spectrum is altered somewhat upon incorporation into the polymer chain. This could lead to a difference in R_o values.

4. Summary

In this paper we introduce a new donor–acceptor dye pair based on the naphthalimide nucleus for energy transfer experiments. These dyes are characterized by a Förster radius $R_o = 3.6$ nm. The dyes can be incorporated into PBMA polymer chains via miniemulsion polymerization. Inspection of GPC traces shows uniform incorporation of the acceptor dye, and a suggestion that, in the absence of chain transfer agent, the donor dye is slightly enriched in the higher molar mass component of the polymer. The particle size distribution for these latex nanoparticles is narrow and dyes do not inhibit the polymerization process.

The unquenched decay profile of the donor dye **4a** in PBMA films showed a small but significant deviation from an exponential decay profile. One of the challenges in this work was the analysis of energy transfer data when the decay profile was not exponential. A model was proposed in which we introduced the mean decay time of the donor and a single R_o value into the analysis. As a test of this model, we examined a series of samples in which free dye was dissolved into a film of the donor-labeled polymer. Analysis of these data gave a fitted value $R_o = 3.8$ nm, close to the value (3.6 nm) obtained by the spectral overlap method.

Acknowledgments

The authors thank Rohm and Haas, Rohm and Haas Canada, and NSERC Canada for their support of this research.

Appendix. Supplementary data

We provide experimental details for the synthesis of the monomers **4a** and **4b**, and for determination of their extinction coefficients at λ_{max}. In addition, we show SEM images (Fig. S1) of sample (PBMA-360^D). Supplementary data associated with this article can be found, in the online version, at doi:10.1016/j.polymer.2007.07.065.

References

[1] Patton TC. In Paint flow and pigment dispersion: a rheological approach to coating and ink technology. John Wiley & Sons; 1979.
[2] (a) Wang Y, Zhao CL, Winnik MA. J Chem Phys 1991;95:2143–53;
(b) Feng J. Ph.D. thesis, University of Toronto; 1996.
(c) Odrobina E. Ph.D. thesis, University of Toronto; 2000.
[3] (a) Zhao CL, Wang YC, Hruska Z, Winnik MA. Macromolecules 1990;23:4082–7;
(b) Liu R, Winnik MA, Stefano FD, Vanketessan J. Macromolecules 2001;34:7306–14.
[4] Oh JK, Wu J, Winnik MA, Craun GP, Rademacher J, Farwaha R. J Polym Sci Part A Polym Chem 2002;40:3001.
[5] Oh JK, Wu J, Winnik MA, Craun GP, Rademacher J, Farwaha R. J Polym Sci Part A Polym Chem 2002;40:1594.
[6] Liu R, Farinha JPS, Winnik MA. Macromolecules 1999;32:3957.
[7] Oh JK, Tomba JP, Ye X, Eley R, Winnik MA, Rademacher J, et al. Macromolecules 2003;36:5804.

[8] Wu J, Tomba JP, Winnik MA, Farwaha R, Rademacher J. Macromolecules 2004;37:4247–53.
[9] Ye X, Wu J, Oh JK, Winnik MA, Wu C. Macromolecules 2003;36:8886–9.
[10] Oh JK, Yang J, Tomba JP, Rademacher J, Farwaha R, Winnik MA. Macromolecules 2003;36:8836–45.
[11] Oh JK, Yang J, Rademacher J, Farwaha R, Winnik MA. Macromolecules 2004;37:5752–61.
[12] Grabtchev I, Philipova T, Meallier P, Guittonneau S. Dyes Pigments 1996;31:31–4.
[13] Asua JM. Prog Polym Sci 2002;27:1283–346.
[14] Antonietti M, Landfester K. Prog Polym Sci 2002;27:689–757.
[15] Chern CS, Liou YC, Chen TJ. Macromol Chem Phys 1998;199:1315–22.
[16] Chern CS, Liou YC. Polymer 1999;40:3763–72.
[17] Chern CS, Chang HT. Eur Polym J 2003;39:1421–9.
[18] Schork FJ, Luo Y, Smulders W, Russum JP, Butté A, Fontenot K. Adv Polym Sci 2005;175:129–255.
[19] Landfester K, Bechthold N, Förster S, Antonietti M. Macromol Rapid Commun 1999;20:81–4.
[20] Landfester K. Macromol Rapid Commun 2001;22:896–936.
[21] Holzapfel V, Musyanovych A, Landfester K, Lorenz MR, Mailänder V. Macromol Chem Phys 2005;206:2440–9.
[22] Bardajee GR, Li AY, Haley JC, Winnik MA. Dyes Pigments, submitted for publication.
[23] Lakowicz JR. Principles of fluorescence spectroscopy. 3rd ed. New York: Springer; 2006.
[24] Lindsey CP, Patterson GD. J Chem Phys 1980;73:3348–57.
[25] Hutchinson RA, Paquet DA, McMinn JH. Macromolecules 1995;28:5655–63.
[26] Chai X-S, Schork FJ, DeCinque A, Wilson K. Ind Eng Chem Res 2005;44:5256–8.
[27] Feng J, Winnik MA. Macromolecules 1997;30:4324–31.
[28] De Gennes P-G. Scaling concepts in polymer physics. Ithaca, NY: Cornell University Press; 1979.
[29] Fredrickson GH. Macromolecules 1986;19:441–7.
[30] Mendelsohn AS, Olvera de la Cruz M, Torkelson JM. Macromolecules 1993;26:6789–99.
[31] Oh JK. Ph.D. thesis, University of Toronto; 2004.